Supplementary Information

The Effect of Organic Cation Dynamics on the Optical Properties in (PEA)$_2$(MA)[Pb$_2$I$_7$] Perovskite Dimorphs

Yulia Lekina,[a,b] Sai S.H. Dintakurti,[c,d] Benny Febriansyah,[e] D.J. Bradley,[d] Jiaxu Yan,[f] Xiangyan Shi,[b] Jason England,[e] Tim White,[g] John V. Hanna,*[d,g] Ze Xiang Shen*[a,b]
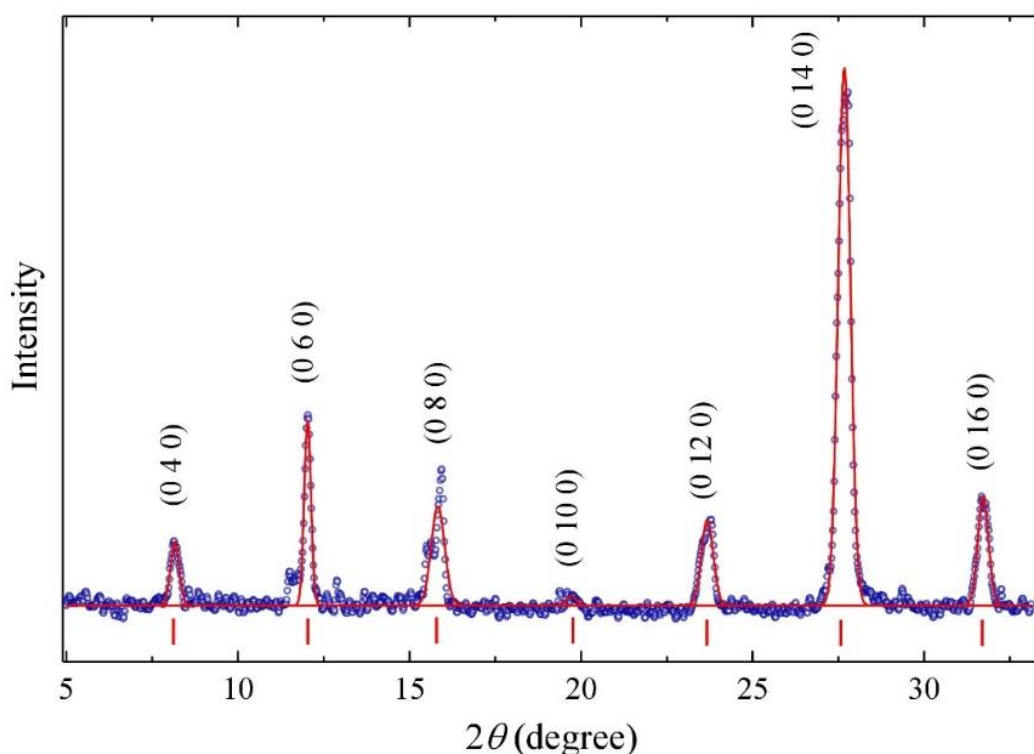
Figure S1. Powder XRD data of the horizontally oriented PEA$_2$MAPb$_2$I$_7$ platelets.

[a.] Centre for Disruptive Photonic Technologies, Nanyang Technological University, 637371, Singapore.

[b.] Division of Physics and Applied Physics, School of Physical and Mathematical Sciences, Nanyang Technological University, 637371, Singapore.

[c.] Interdisciplinary Graduate School (IGS), Nanyang Technological University, 50 Nanyang Avenue, Singapore 639798, Singapore.

[d.] Department of Physics, University of Warwick, Gibbet Hill Rd., Coventry CV4 7AL, UK

[e.] Division of Chemistry and Biological Chemistry, School of Physical and Mathematical Sciences, Nanyang Technological University, 21 Nanyang Link, Singapore 637371, Singapore.

[f.] Key Laboratory of Flexible Electronics (KLOFE) & Institute of Advanced Materials (IAM), Jiangsu National Synergistic Innovation Center for Advanced Materials (SICAM), Nanjing Tech University (Nanjing Tech), Nanjing 211816, China.

[g.] School of Materials Science and Engineering, Nanyang Technological University, 50 Nanyang Avenue, Singapore 639798, Singapore
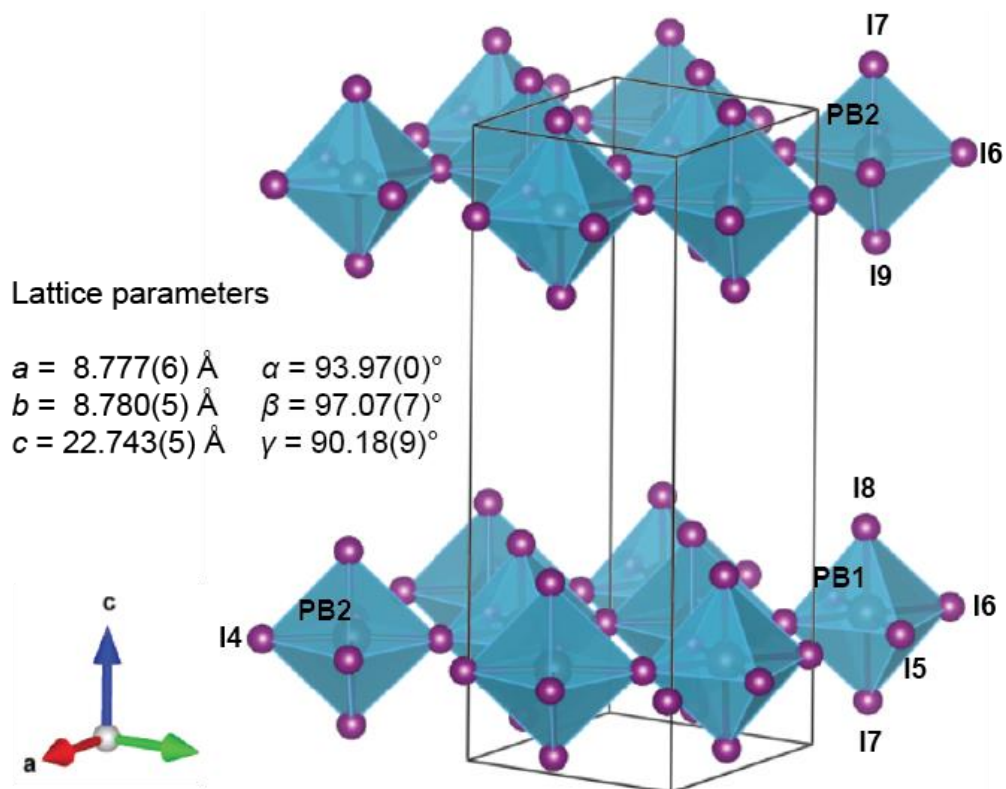
Figure S2. Structure (PEA)$_2$(MA)[Pb$_2$I$_7$] obtained by single crystal X-Ray analysis and unit cell parameters. Only coordinates of inorganic atoms were determined.

Table S1. Refined positions and equivalent isotropic atomic displacement parameters obtained from best fit single crystal structural model.

Atom site	x	y	z	U_{eq} (Å^3)
PB1	0.29527(9)	0.77484(9)	0.14482(4)	0.0336(3)
PB2	0.79762(9)	0.27700(9)	0.14486(4)	0.0334(3)
I3	0.4915(2)	0.0771(2)	0.14074(9)	0.0526(5)
I4	-0.0076(2)	0.9730(2)	0.14142(9)	0.0549(5)
I5	0.0991(2)	0.4709(2)	0.14172(10)	0.0616(5)
I6	0.5973(2)	0.5774(2)	0.14138(9)	0.0551(5)
I7	0.2496(2)	0.7522(2)	0.00021(7)	0.0566(5)
I8	0.3507(3)	0.8041(3)	0.28379(9)	0.0626(5)
I9	0.8403(3)	0.2885(3)	0.28374(9)	0.0622(5)

(a) *anti* conformers *gauche* conformers

out-of-plane

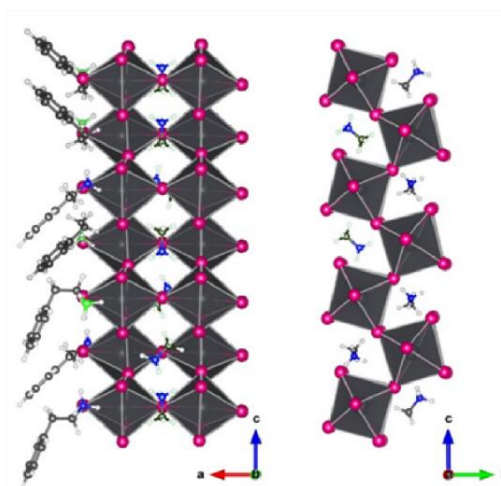out-of-plane

in-plane
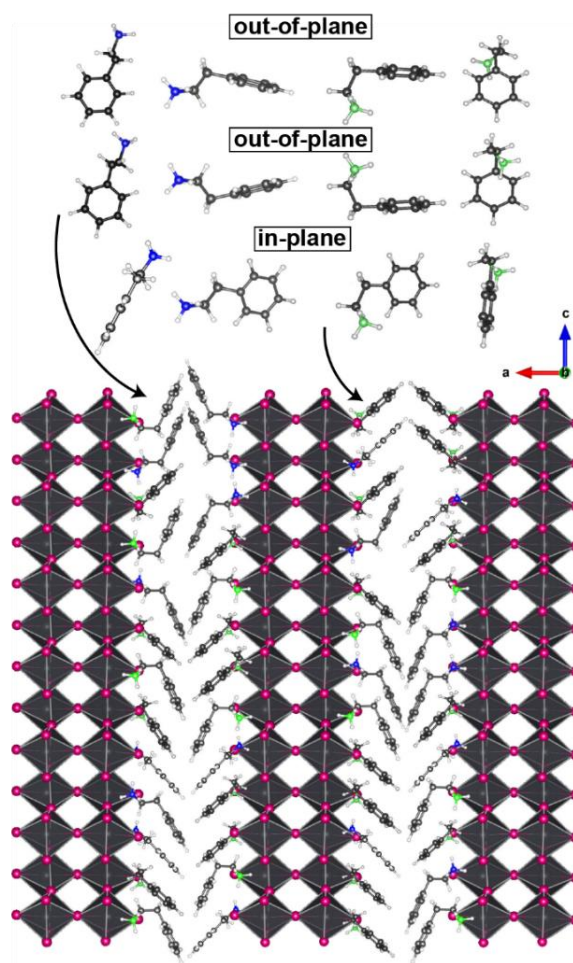
(b)

Figure S3. Schematic representations of the structural disorder in the organic sublattice as in incurred (a) by the PEA$^+$ cations in the 2D interlayer channels, and (b) by the MA$^+$ cations in the octahedral cavities.
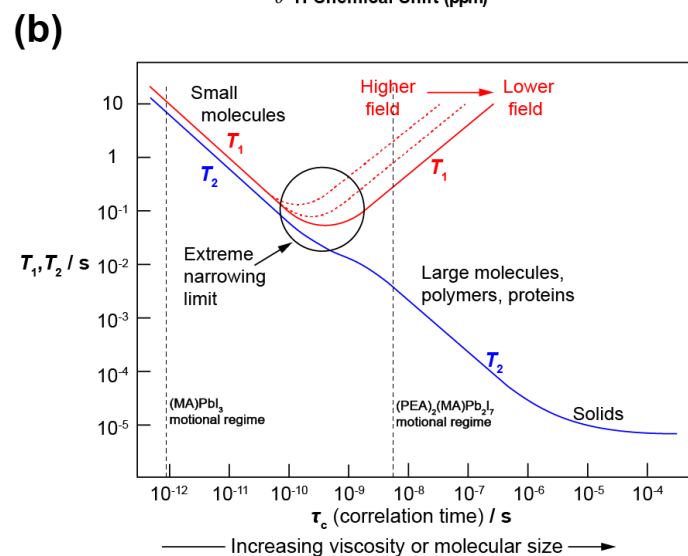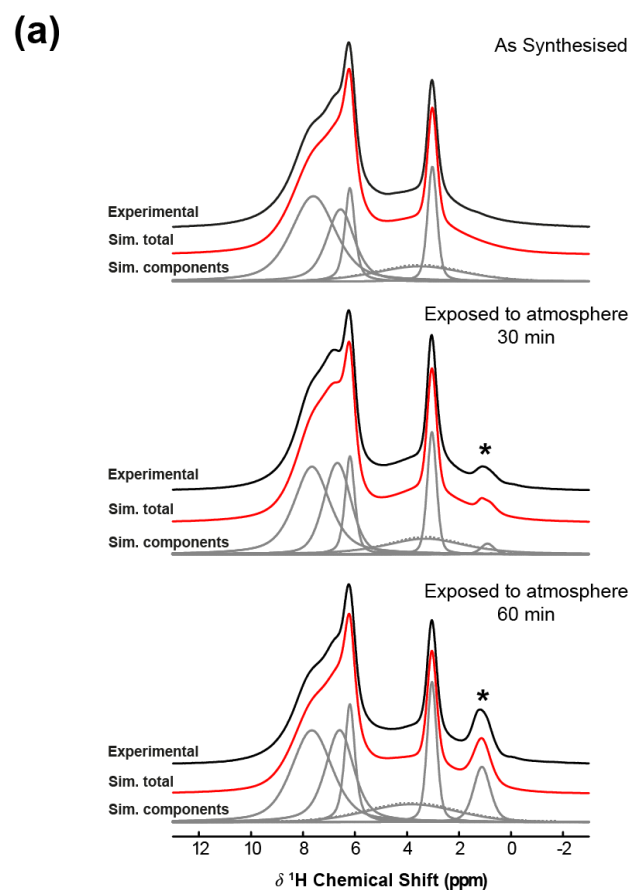
(a)

(b)

Figure S4. Additional ^{1}H MAS NMR characterisation of the $(PEA)_2(MA)[Pb_2I_7]$ system showing, (a) spectral evidence for H_2O absorption (H_2O resonance marked with an asterisk, $\nu_0 = 800.16$ MHz, $\nu_r = 35$ kHz) commensurate with increasing times of atmospheric exposure, and (b) mapping of the motional regime of the PEA^+ and MA^+ cations according the relationship between the ^{1}H T_1 and T_2 relaxation times.
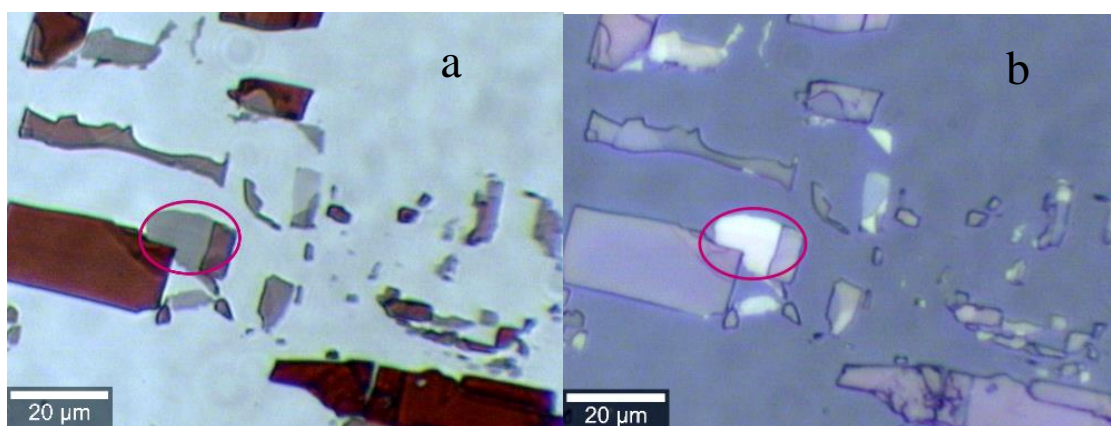
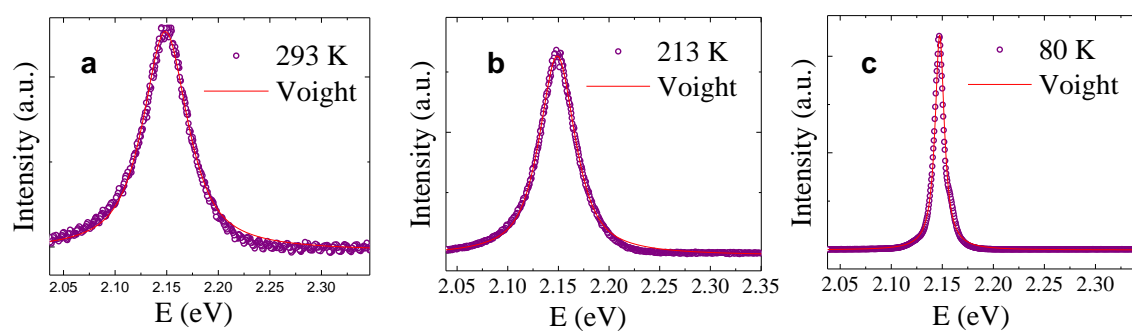Figure S5. Optical images of the exfoliated crystal a) in transmission light, b) in reflected light.

Figure S6. Fitting of PL spectra of (PEA)$_2$(MA)[Pb$_2$I$_7$] using one Pseudo-Voight component.
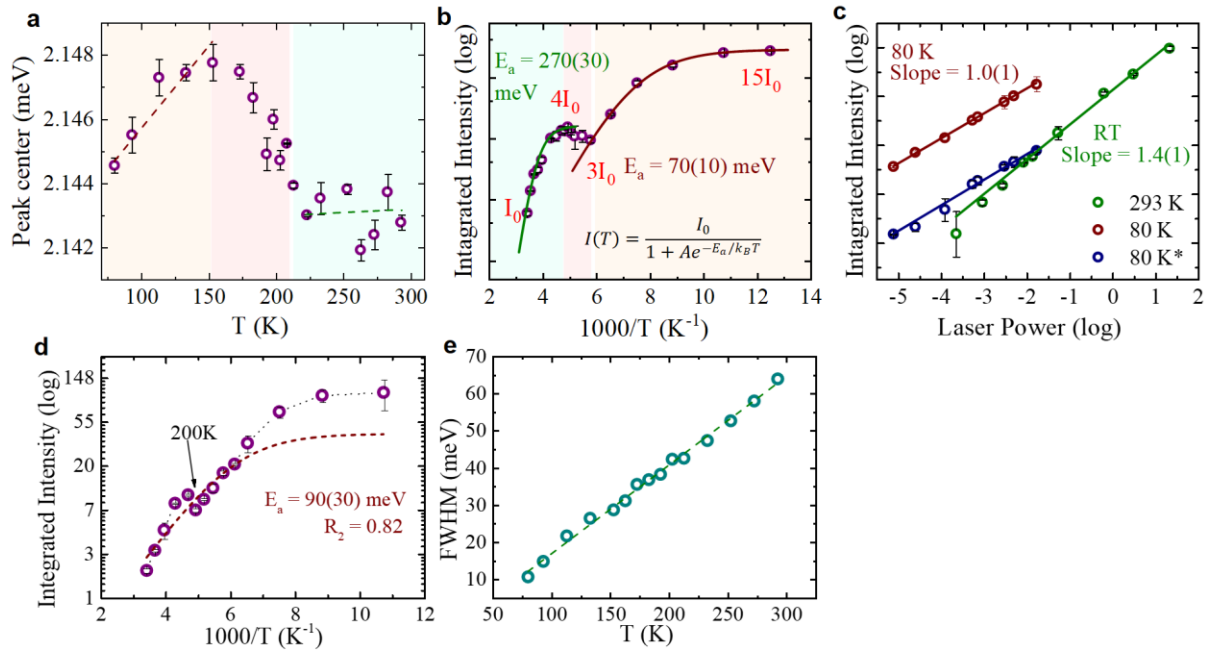
Figure S7. Temperature dependent (heating from 80K to 300 K) PL response under 457 nm excitation showing, (a) PL peak position vs temperature, (b) dependence of integrated PL intensity (logarithmic scale) vs 1/T and the fit of these data using $I = \mathrm{I}_0 / \left(1 + exp\left(-\frac{E_a}{k_b}\frac{1}{T}\right)\right)$, (c) excitation intensity dependence of integrated PL intensity (bilogarithmic scale) vs laser power (green points correspond to RT measurements, brown points represent the main component, blue points represent an additional component at low temperature), (d) integrated PL intensity vs 1/T under 457 nm excitation (cooling from 300 to 80K) where a fit of the whole range is presented, (e) full-width-half-maximum (FWHM) of the PL data from the $(PEA)_2(MA)[Pb_2I_7]$ systems as a function of temperature.
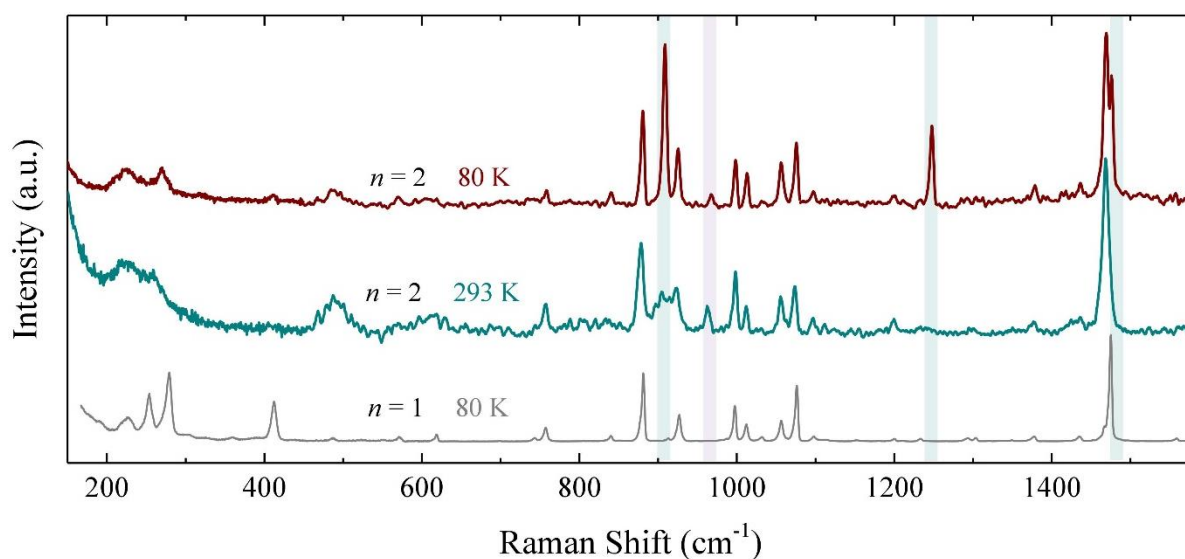
Figure S8. Raman data from $(PEA)_2[PbI_4]$ (n = 1) hybrid perovskite system at 80 K (bottom), and the $(PEA)_2(MA)[Pb_2I_7]$ (n = 2) system at room temperature and at 80 K. The $(PEA)_2[PbI_4]$ spectrum is shown for comparison as the framework charge is balanced by PEA$^+$ cations only. This provides clear evidence that the highlighted peaks appearing in the $(PEA)_2(MA)[Pb_2I_7]$ (n = 2) spectrum yet absent from the $(PEA)_2[PbI_4]$ (n = 1) spectrum correspond to MA$^+$ modes. From these data, only the peaks assigned to MA$^+$ cation vibrations exhibit a strong temperature dependence.
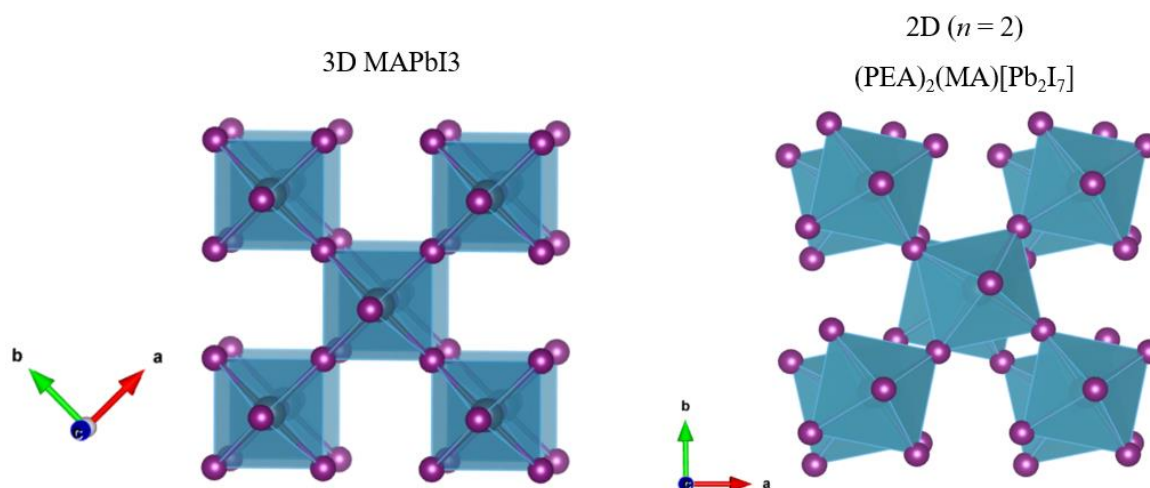

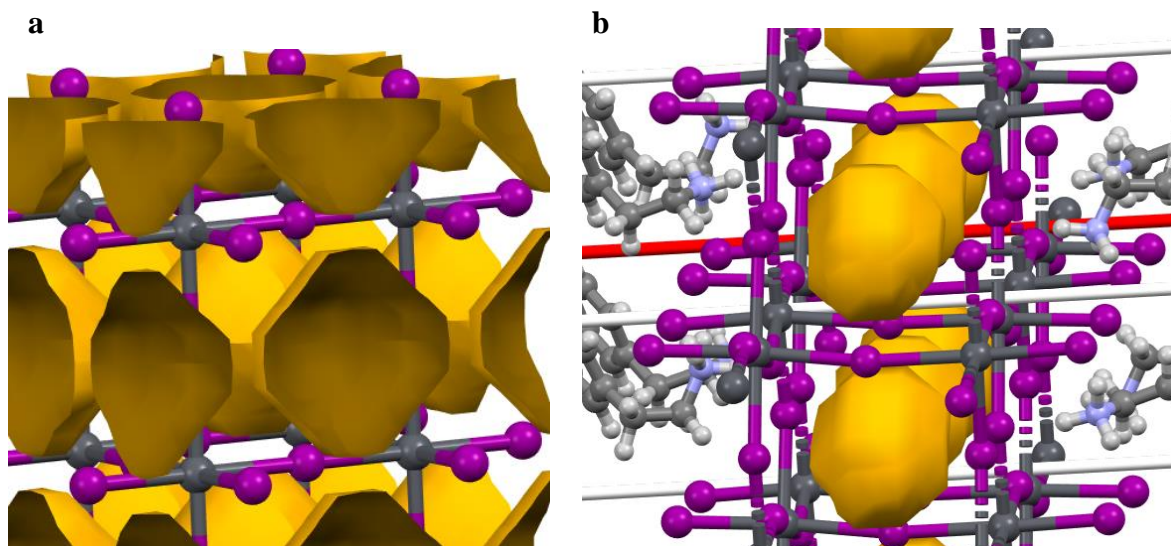Figure S9. Representations of the inorganic sublattices in 3D (P4mm) and 2D (P1) perovskites.

Figure S10. The MA$^+$ cavities is a) MAPbI$_3$ in the tetragonal phase at room temperature (volume = 78.5 Å^3), b) in (PEA)$_2$(MA)[Pb$_2$I$_7$] at room temperature (volume = 59.1 Å^3). The voids are calculated by means of Mercury software with the following parameters: Probe Radius = 1.8 (MA$^+$ ionic radius), Grid Spacing = 0.7.